IOSR Journal of Applied Physics (IOSR-JAP)
e-ISSN: 2278-4861.Volume 18, Issue 4 Ser. 1 (Jul. – Aug. 2026), PP 56-63
www.iosrjournals.org

Spectral, Thermal and Photoluminescence Properties of Ho^{3+}doped Tellurite Glasses with Large Balaji-Shankar Relation

S.L. Meena
Ceramic Laboratory, Department of physics, Jai Narain Vyas University, Jodhpur 342001(Raj.) India

Abstract
Glasses samples containing Ho^{3+} in Yttrium Zinc Lithium Lead Sodalime Borotellurite Glasses (25-x)TeO_2: 10ZnO: 10Li_2O: 10PbO: 10Na_2O: 10CaO: 10Y_2O_3 :15B_2O_3 :xHo_2O_3 (where x=1, 1.5,2 mol %) have been prepared by melt-quenching method. The amorphous nature of the prepared glass samples was confirmed by X-ray diffraction. Optical absorption, Excitation and fluorescence spectra were recorded at room temperature for all glass samples. The thermal parameters were calculated using DTA Thermogram. Judd-Ofelt intensity parameters Ω_λ (λ=2, 4 and 6) are evaluated from the intensities of various absorption bands of optical absorption spectra. Using these intensity parameters various radiative properties like spontaneous emission probability (A), branching ratio (β), radiative life time (τ_R) and stimulated emission cross–section (σ_p) of various emission lines have been evaluated.

Keywords: *YZLLSLBT Glasses, Thermal Properties, Judd-Ofelt Theory, Optical Properties, Photoluminescence Properties.*

I. Introduction

Rare earth glasses have attracted much attention, because they have many applications such as electro-luminescent devices, memory devices optical fibers, sensors, glass lasers, optical fiber amplifiers, up-conversion lasers, waveguide laser and optical fiber amplifiers [1–5].Among different glasses tellurite glasses have unique properties. They have high refractive index, high density, high transparency, high ultraviolet transmission, low dispersion rates and large value of thermal parameters [6-8]. Tellurite glasses have good chemical and mechanical properties [9-12]. The addition of network modifier (NWF) Li_2O is to improve both mechanical and electrical properties of such glasses. Zinc oxide is added in the glass matrix to increase glass forming ability and to ensure low rates of crystallization in the glass system [13-16].Addition of heavy metal oxide PbO is expected to make these glasses more moisture resistant, high chemical and thermal stability due to its dual role, one as a glass former and the other as a modifier. Among active rare-earth ions Ho^{3+} exhibits high solubility in ceramic glasses, which also possess excellent Thermal and optical properties [17, 18].Recently tellurite based glasses have a wide range of potential applications in laser technologies, optical data transmission, detection, photonic and sensing applications [19-22].

The present work reports on the preparation and characterization of rare earth doped heavy metal oxide (HMO) glass systems for lasing materials. I have studied on the Optical absorption, Excitation, fluorescence and Thermal spectra of Ho^{3+} doped yttrium zinc lithium lead sodalime borotellurite glasses. The glass transition temperature (T_g), onset crystallization temperature (T_c), crystallization temperature (T_p), melting temperature(T_m), thermal stability (T_s),Balaji Parameter (B_P),Hurbe's criterion (H_R),reduced glass transition temperature (T_{rg}) and Shankar parameter were calculated using DTA Thermogram. The intensities of the transitions for the rare earth ions have been estimated successfully using the Judd-Ofelt theory, The laser parameters such as radiative probabilities(A),branching ratio (β), radiative life time(τ_R) and stimulated emission cross section(σ_p) are evaluated using J.O.intensity parameters(Ω_λ, λ=2,4 and 6).

II. Experimental Techniques

Preparation of glasses

The following Ho^{3+}doped borate glass samples (25-x)TeO_2: 10ZnO: 10Li_2O: 10PbO: 10Na_2O: 10CaO: 10Y_2O_3 :15B_2O_3 :xHo_2O_3 (where x=1,1.5 and 2 mol%) have been prepared by melt-quenching method. Analytical reagent grade chemical used in the present study consist of TeO_2, ZnO, Li_2O, PbO, Na_2O, CaO,Y_2O_3, B_2O_3 and Ho_2O_3. They were thoroughly mixed by using an agate pestle mortar. then melted at 1060^0C by an electrical muffle furnace for 2h., After complete melting, the melts were quickly poured in to a preheated stainless steel mould and annealed at temperature of 250^0C for 2h to remove thermal strains and stresses. Every

time fine powder of cerium oxide was used for polishing the samples. The glass samples so prepared were of good optical quality and were transparent. The chemical compositions of the glasses with the name of samples are summarized in **Table 1.**

Table 1.

Chemical composition of the glasses

Sample	Glass composition (mol %)
YZLLSLBT (UD)	**$25TeO_2$: 10ZnO: $10Li_2O$: 10PbO: $10Na_2O$: 10CaO: $10Y_2O_3$:$15B_2O_3$**
YZLLSLBT HO(1.0)	**$24TeO_2$: 10ZnO: $10Li_2O$: 10PbO: $10Na_2O$: 10CaO: $10Y_2O_3$:$15B_2O_3$:$1Ho_2O_3$**
YZLLSLBT HO(1.5)	**$23.5TeO_2$: 10ZnO: $10Li_2O$: 10PbO: $10Na_2O$: 10CaO: $10Y_2O_3$:$15B_2O_3$:1.5 Ho_2O_3**
YZLLSLBT HO(2.0)	**$23TeO_2$: 10ZnO: $10Li_2O$: 10PbO: $10Na_2O$: 10CaO: $10Y_2O_3$:$15B_2O_3$:2 Ho_2O_3**

YZLLSLBT (UD) -Represents undoped Yttrium Zinc Lithium Lead Sodalime Borotellurite glass specimen.
YZLLSLBT (HO)-Represents Ho^{3+} doped Yttrium Zinc Lithium Lead Sodalime Borotellurite glass specimens.

III. Theory

3.1 Oscillator Strength

The intensity of spectral lines are expressed in terms of oscillator strengths using the relation [23].

$$f_{expt.} = 4.318 \times 10^{-9} \int \varepsilon(\nu)\, d\nu \qquad (1)$$

where, $\varepsilon(\nu)$ is molar absorption coefficient at a given energy ν (cm^{-1}), to be evaluated from Beer–Lambert law. Under Gaussian Approximation, using Beer–Lambert law, the observed oscillator strengths of the absorption bands have been experimentally calculated [24], using the modified relation:

$$P_m = 4.6 \times 10^{-9} \times \frac{1}{cl} \log \frac{I_0}{I} \times \Delta\upsilon_{1/2} \qquad (2)$$

where c is the molar concentration of the absorbing ion per unit volume, I is the optical path length, $\log I_0/I$ is optical density and $\Delta\upsilon_{1/2}$ is half band width.

3.2. Judd-Ofelt Intensity Parameters

According to Judd [25] and Ofelt [26] theory, independently derived expression for the oscillator strength of the induced forced electric dipole transitions between an initial J manifold $|4f^N (S, L) J>$ level and the terminal J' manifold $|4f^N (S',L') J'>$ is given by:

$$\frac{8\Pi^2 mc\bar{\upsilon}}{3h(2J+1)} \frac{1}{n}\left[\frac{(n^2+2)^2}{9}\right] \times S(J, J') \qquad (3)$$

Where, the line strength S (J, J') is given by the equation

$$S(J, J') = e^2 \sum_{\lambda=2,4,6} \Omega_\lambda \langle 4f^N(S, L)\, J \| U^{(\lambda)} \| 4f^N(S', L')\, J' \rangle^2 \qquad (4)$$

In the above equation m is the mass of an electron, c is the velocity of light, ν is the wave number of the transition, h is Planck's constant, n is the refractive index, J and J' are the total angular momentum of the initial and final level respectively, Ω_λ (λ=2,4and 6) are known as Judd-Ofelt intensity.

3.3 Radiative Properties

The Ω_λ parameters obtained using the absorption spectral results have been used to predict radiative properties such as spontaneous emission probability (A) and radiative life time (τ_R), and laser parameters like fluorescence branching ratio (β_R) and stimulated emission cross section (σ_p).

The spontaneous emission probability from initial manifold $|4f^N (S', L') J'>$ to a final manifold $|4f^N (S, L) J>|$ is given by:

$$A[(S', L') J'; (S, L) J] = \frac{64\pi^2\nu^3}{3h(2J'+1)}\left[\frac{n(n^2+2)^2}{9}\right] \times S(J', \bar{J}) \qquad (5)$$

Where, $S(J', J) = e^2 [\Omega_2 \| U^{(2)} \|^2 + \Omega_4 \| U^{(4)} \|^2 + \Omega_6 \| U^{(6)} \|^2]$

The fluorescence branching ratio for the transitions originating from a specific initial manifold $|4f^N (S', L') J'>$ to a final many fold $|4f^N (S, L) J >$ is given by

$$\beta [(S', L') J'; (S, L) J] = \sum_{S L J} \frac{A[(S' L)]}{A[(S' L') J' (\bar{S} \bar{L})]} \quad (6)$$

where, the sum is over all terminal manifolds.

The radiative life time is given by

$$\tau_{rad} = \sum_{S L J} A[(S', L') J'; (S, L)] = A_{Total}^{-1} \quad (7)$$

where, the sum is over all possible terminal manifolds. The stimulated emission cross -section for a transition from an initial manifold $|4f^N (S', L') J'>$ to a final manifold $|4f^N (S, L) J >|$ is expressed as

$$\sigma_p(\lambda_p) = \left[\frac{\lambda_p^4}{8\pi c n^2 \Delta\lambda_{eff}}\right] \times A[(S', L') J'; (\bar{S}, \bar{L}) \bar{J}] \quad (8)$$

where, λ_p the peak fluorescence wavelength of the emission band and $\Delta\lambda_{eff}$ is the effective fluorescence line width.

3.4 Nephelauxetic Ratio (β') and Bonding Parameter ($b^{1/2}$)

The nature of the R-O bond is known by the Nephelauxetic Ratio (β') and Bonding Parameters ($b^{1/2}$), which are computed by using following formulae [27, 28]. The Nephelauxetic Ratio is given by

$$\beta' = \frac{\nu_g}{\nu_a} \quad (9)$$

where, ν_a and ν_g refer to the energies of the corresponding transition in the glass and free ion, respectively. The value of bonding parameter ($b^{1/2}$) is given by

$$b^{1/2} = \left[\frac{1-\beta'}{2}\right]^{1/2} \quad (10)$$

IV. Result and Discussion

4.1 XRD Measurement

Figure 1 presents the XRD pattern of the sample contain – TeO_2 which is show no sharp Bragg's peak, but only a broad diffuse hump around low angle region. This is the clear indication of amorphous nature within the resolution limit of XRD instrument.

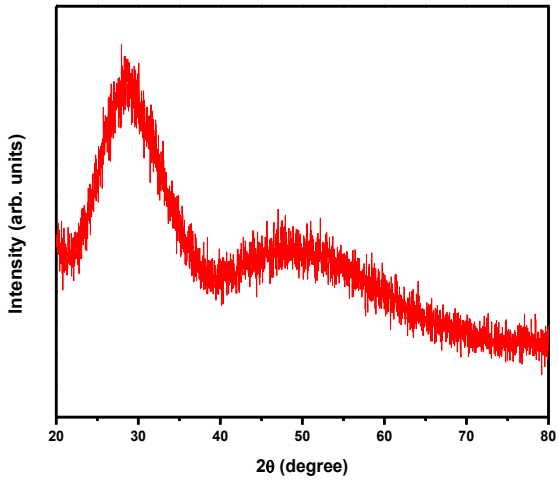

Fig. 1: X-ray diffraction pattern of YZLLSLBT HO (1.0) glass.

4.2 Thermal Property

Differential thermal analysis checks the heat absorbed by glass samples during heating or cooling. Fig. 2 depicts the DTA thermogram of powdered YZLLSLBT sample. The glass transition temperature (T_g), onset crystallization temperature (T_c), crystallization temperature (T_p), melting temperature(T_m), thermal stability (T_s),Balaji Parameter (B_P), Hurbe's criterion (H_R) and reduced glass transition temperature (T_{rg}) were calculated. Shankar's parameter also calculated by using eq. (13). All the determined thermal parameters are given in table 2.

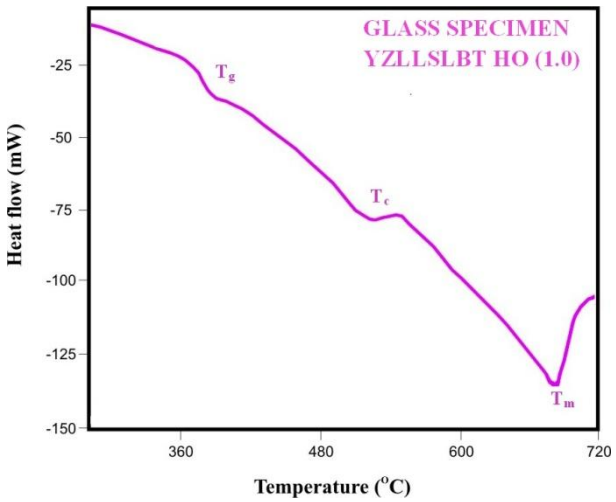

Fig.2: DTA curve of YZLLSLBT HO (1.0) glass.

Table 2. Thermal parameters determined from the DTA traces of YZLLSLBT HO glasses.

Sample Name	T_g (^{0}C)	T_c(^{0}C)	T_p(^{0}C)	T_m(^{0}C)	T_s(^{0}C)	B_P(^{0}C)	H_R(^{0}C)	K_S(^{0}C)	T_{rg}(^{0}C)	$B_P \times K_S$
YZLLSLBT HO (1.0)	375	512	550	685	137	3.605	0.220	34.600	0.547	124.733
YZLLSLBT HO (1.5)	380	513	553	687	133	3.325	0.230	33.686	0.553	112.006
YZLLSLBT HO (2.0)	385	515	555	696	130	3.250	0.229	32.971	0.558	107.156

The thermal stability of the glass samples can be calculated by difference between onset crystallization temperature and transition temperature [29].

Thermal Stability (T_s)= T_c-T_g (11)

Balaji Parameter can be calculated using [29].

Balaji Parameter (B_P) = $[(T_c-T_g)/(T_p-T_c)]$ (12)

Hruby's criterion is calculated using the Hurby's relation [29].

Hruby's criterion(H_R)=$[(T_p-T_c)/(T_m-T_c)]$ (13)

Reduced glass transition temperature is given as [29].

Reduced glass transition temperature (T_{rg}) =T_g/T_m (14)

Shankar Parameter is given as [29].

K_S= $[(T_m-T_c)\ (T_c-T_g)/T_m]$ (15)

Balaji-Shankar relation is given by

$$(B_P \times K_S) = [(T_c - T_g)^2 (T_m - T_c) / T_m(T_p - T_c)] \quad (16)$$

4.3 Absorption Spectrum

The absorption spectra of Ho^{3+}doped YZLLSLBT HO(1.0) glass specimen has been presented in Figure 3 in terms of optical density versus wavelength. Twelve absorption bands have been observed from the ground state $^5I_8$ to excited states $^5I_5$, $^5I_4$, $^5F_5$, $^5F_4$, $^5F_3$, $^3K_8$, $^5G_6$, $(^5G,^3G)_5$, $^5G_4$, $^5G_2$, $^5G_3$, and$^3F_4$ for Ho^{3+} doped YZLLSLBT HO(1.0) glass.

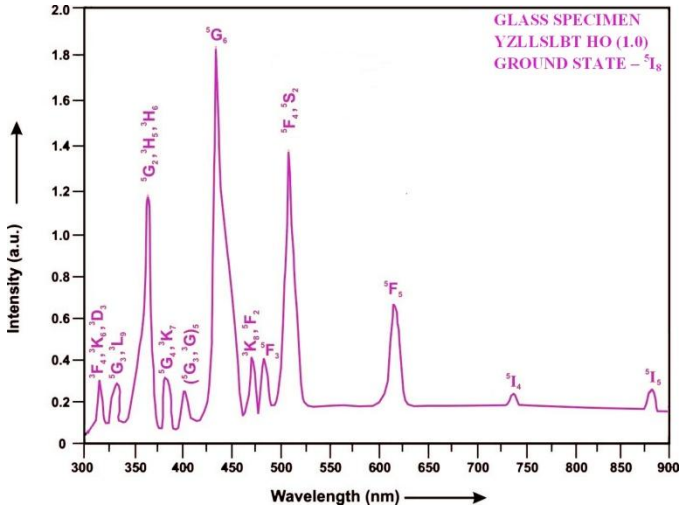

Fig. 3: Absorption spectrum of YZLLSLBT HO (1.0) glass.

The experimental and calculated oscillator strength for Ho^{3+} ions in YZLLSLBT glasses are given in **Table 3.**

Table 3: Measured and calculated oscillator strength ($P_m \times 10^{+6}$) of Ho^{3+}ions in YZLLSLBT glasses.

Energy level from $^5I_8$	Glass YZLLSLBT HO(1.0)		Glass YZLLSLBT HO(1.5)		Glass YZLLSLBT HO(2.0)	
	$P_{exp.}$	$P_{cal.}$	$P_{exp.}$	$P_{cal.}$	$P_{exp.}$	$P_{cal.}$
$^5I_5$	0.45	0.24	0.42	0.24	0.38	0.24
$^5I_4$	0.07	0.02	0.06	0.02	0.05	0.02
$^5F_5$	3.68	2.82	3.64	2.79	3.60	2.76
$^5F_4$	4.70	4.37	4.65	4.32	4.59	4.27
$^5F_3$	1.58	2.43	1.54	2.40	1.50	2.37
$^3K_8$	1.46	1.99	1.42	1.96	1.39	1.93
$^5G_6$	25.64	25.62	24.72	24.71	23.65	23.66
$(^5G,^3G)_5$	3.85	1.73	3.82	1.71	3.79	1.69
$^5G_4$	0.08	0.62	0.07	0.61	0.06	0.60
$^5G_2$	5.72	5.45	5.67	5.28	5.62	5.08
$^5G_3$	1.53	1.40	1.49	1.38	1.45	1.35
$^3F_4$	1.42	4.23	1.39	4.19	1.34	4.13
r.m.s. deviation	±1.1053		±1.1033		±1.1050	

Computed values of F_2, Lande′ parameter (ξ_{4f}), Nephlauxetic ratio (β') and bonding parameter ($b^{1/2}$) for Ho^{3+} ions in YZLLSLBT glass specimen are given in Table 4.

Table 4: F_2, ξ_{4f}, β' and $b^{1/2}$ parameters for Holmium doped glass specimen.

Glass Specimen	F_2	ξ_{4f}	β'	$b^{1/2}$
Ho^{3+}	358.82	1258.16	0.9337	0.1821

The values of Judd-Ofelt intensity parameters are given in **Table 5.**

Table 5: Judd-Ofelt intensity parameters for Ho^{3+} doped YZLLSLBT glass specimens.

Glass Specimen	$\Omega_2(pm^2)$	$\Omega_4(pm^2)$	$\Omega_6(pm^2)$	Ω_4/Ω_6	Ref.
YZLLSLBT HO (1.0)	6.489	1.423	2.304	0.6176	P.W.
YZLLSLBT HO (1.5)	6.217	1.409	2.276	0.6191	P.W.
YZLLSLBT HO (2.0)	5.904	1.389	2.246	0.6184	P.W.
Tellurite	4.980	0.990	2.960	0.3345	[30].
ZLCBS (HO)	5.674	1.205	2.005	0.6010	[31].
ZLSLCBS (HO)	5.713	1.332	2.181	0.6107	[32].

4.4 Excitation Spectrum

The Excitation spectrum of YZLLSLBT (HO 01) glass has been presented in Figure 4 in terms of Excitation Intensity versus wavelength. The excitation spectrum was recorded in the spectral region 325–525 nm fluorescence at 545nm having different excitation band centered at 349,419, 452, 473and 486 nm are attributed to the $^5G_3$, (^5G, $^3G)_5$, $^5G_6$, $^3K_8$ and $^5F_3$ transitions, respectively. The highest absorption level is $^5G_6$ and is at 452nm.So this is to be chosen for excitation wavelength.

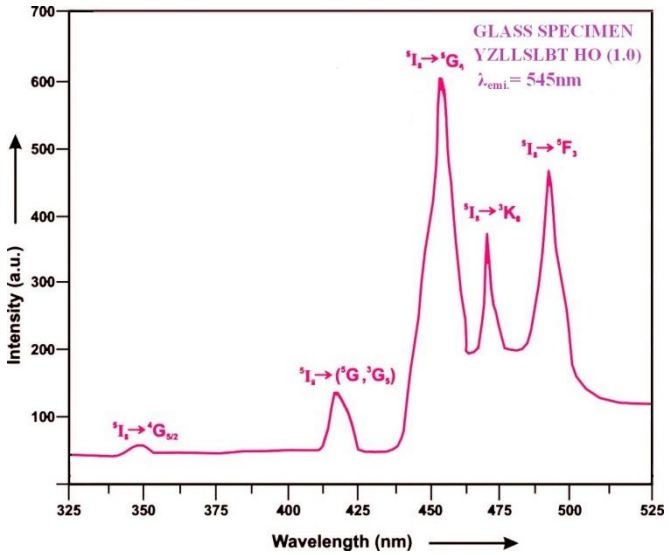

Fig. 4: Excitation spectrum of YZLLSLBT HO (1.0) glass.

4.5 Fluorescence Spectrum

The fluorescence spectrum of Ho^{3+}doped in Yttrium Zinc Lithium Lead Sodalime Borotellurite glass is shown in Figure 5. There are eleven broad bands observed in the Fluorescence spectrum of Ho^{3+}doped Yttrium Zinc Lithium Lead Sodalime Borotellurite glass. The wavelengths of these bands along with their assignments are given in Table 6. The peak with maximum emission intensity appears at 2035 nm and corresponds to the ($^5I_7 \rightarrow {}^5I_8$) transition.

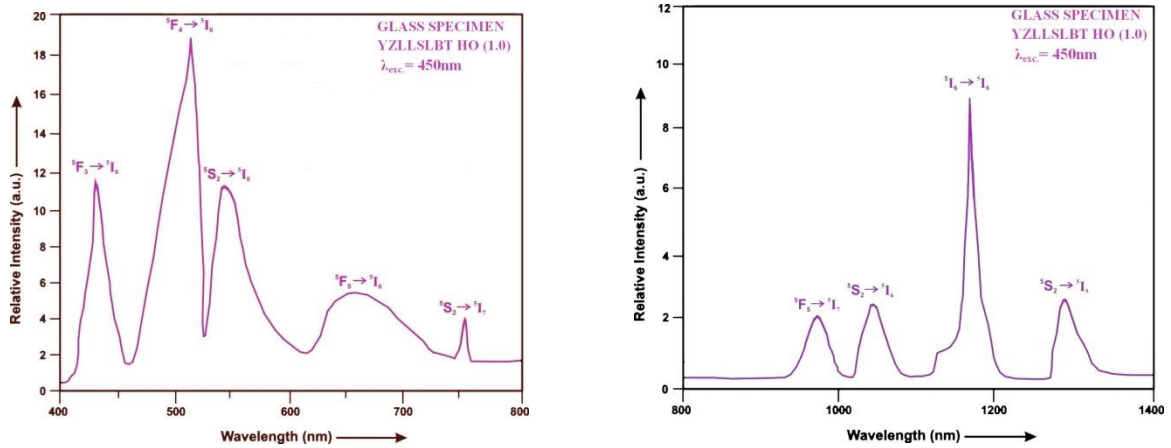

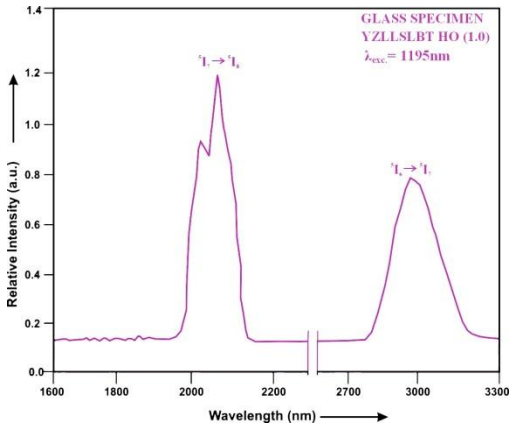

Fig. 5: Fluorescence spectrum of YZLLSLBT HO (1.0) glass.

Table6: Emission peak wave lengths (λ_p),radiative transition probability (A_{rad}),branching ratio (β),stimulated emission cross-section(σ_p) and radiative life time(τ_R) for various transitions in Ho^{3+} doped YZLLSLBT glasses.

Transition		YZLLSLBT HO(1.0)				YZLLSLBT HO(1.5)				YZLLSLBT HO(2.0)			
	λ_{max} (nm)	$A_{rad}(s^{-1})$	β	σ_p (10^{-20} cm^2)	τ_R(μs)	$A_{rad}(s^{-1})$	β	σ_p (10^{-20} cm^2)	τ_R (μs)	$A_{rad}(s^{-1})$	β	σ_p (10^{-20} cm^2)	τ_R (10^{-20} cm^2)
$^5F_3 \rightarrow {}^5I_8$	435	3958.598	0.2474	0.565		3918.35	0.2473	0.542		3874.49	0.2474	0.522	
$^5F_4 \rightarrow {}^5I_8$	501	6330.75	0.3956	1.202		6268.42	0.3957	1.160		6197.38	0.3957	1.126	
$^5S_2 \rightarrow {}^5I_8$	555	1652.36	0.1033	0.441		1635.57	0.1032	0.427		1617.26	0.1032	0.414	
$^5F_5 \rightarrow {}^5I_8$	652	1803.40	0.1127	0.720		1786.39	0.1128	0.700		1765.82	0.1127	0.679	
$^5S_2 \rightarrow {}^5I_7$	761	1258.49	0.0786	1.078	6249.06	1245.70	0.0786	1.050	6312.29	1231.75	0.0786	1.016	6385.07
$^5F_5 \rightarrow {}^5I_7$	995	418.57	0.0262	1.181		413.61	0.0261	1.139		407.67	0.0260	1.103	
$^5I_6 \rightarrow {}^5I_8$	1032	192.45	0.0120	0.684		190.54	0.0120	0.664		188.39	0.0120	0.644	
$^5S_2 \rightarrow {}^5I_5$	1195	219.80	0.0137	1.188		217.36	0.0137	1.155		214.66	0.0137	1.127	
$^5S_2 \rightarrow {}^5I_6$	1310	58.59	0.0037	0.601		57.99	0.0037	0.582		57.34	0.0037	0.563	
$^5I_7 \rightarrow {}^5I_8$	2035	87.18	0.0054	4.523		86.20	0.0054	4.360		85.10	0.0054	4.224	
$^5I_6 \rightarrow {}^5I_7$	2925	22.26	0.0014	3.883		21.98	0.0014	3.776		21.67	0.0014	3.645	

V. Conclusion

In the present study, the glass samples of composition (25-x)TeO_2: 10ZnO: 10Li_2O: 10PbO: 10Na_2O: 10CaO: 10Y_2O_3 :15B_2O_3 :xHo_2O_3 (where x =1, 1.5and 2mol %) have been prepared by melt-quenching method. The value of Balaji-Shankar relation is found to be greater than 100 ^{0}C, which indicates that the prepared glass samples have good thermal stability. The value of stimulated emission cross-section (σ_p) is found to be maximum for the transition ($^5I_7 \rightarrow {}^5I_8$) for glass YZLLSLBT HO (1.0), suggesting that glass YZLLSLBT HO (1.0) is better compared to the other two glass systems YZLLSLBT HO (1.5)and YZLLSLBT HO (2.0). The large stimulated emission cross section in borate glasses suggests the possibility of utilizing these systems as laser materials. The results show that the Ho^{3+} doped borotellurite glasses could be potential candidates for Thermionic and NIR light emission applications.

References

[1].Meena,S.L.(2026).Spectral and Thermal Properties of Dy^{3+} ions doped Zinc Lithium Sodalime Potassiumniobate Bismuthborate Glasses

[2]. Marzouk,M.A.,Khattab,R.M.,Sadek,H.E.H.,Ali,M.M.,Ali,I.S.(2025).Sustainable synthesis and characterization of Bi_2O_3 doped borate glass-ceramics from granite sludge waste with emphasis on structure,luminescence and mechanical properties,J.Ino.Org.Poly.Mat.35,9719-9735.

[3].Meena, S.L. (2025). Spectral and Thermal properties of Eu^{3+} doped Ytterium Zinc Lithium Alumina Tungsten Potassiumniobate Bismuth Borate Glasses with low Hruby's criterion, IOSR Appl.Phys.17,48-54.

[4].Arora,R.,Kaur,N.,Singh,H.,Kumar,D.,Bhatia,V.,Singh,S.P.(2024).B_2O_3-TeO_2-ZnO-Na_2O-Nd_2O_3 glass matrices: A comprehensive study of physical,structural,optical and thermoluminescence properties,Mater.Chem.Phys.313,128783.

[5].Meena,S.L.(2024).Structural,physical and optical properties of Pr^{3+} doped in bismuth borate glasses,Appl.Phys.A,404,1-12.

[6].Meena,S.L.(2023).Spectral and Raman analysis of Er^{3+} doped ytterbium zinc lithium sodalime magnesium borophosphate glasses,Int.Inn.Res.Sci.Eng.Tech.12,10915-24.

[7].Mahraz,Z.A.S.,Sazali,E.,Sahar,M.,Amran,N.U.,Yaacob,S.,Aziz,S.M.,Mawlud,S.,Noor,F.,Harun,A.(2019).Spectroscopic inestigations of near-infrared emission from Nd^{3+} doped zinc phosphate glasses, Judd-Ofelt evaluation,J.Non-Cryst.Solids,509,106-114.

[8].Meena, S.L. (2022). Spectral and Up conversion Properties of Dy^{3+} ions doped Zinc Lithium Potessiumniobate Borosilicate Glasses,Int.Eng.Sci.Inv.11, 44-49.

[9].Sailaja,P.,Mahamuda,Sk.,Dedeepya,G.,Alzahrani,J.S.,Swapna,K.,Venkateswarlu,M.,Rao,A.S.,Alrowaili,Z.A.,Olarinoye,I.O.,Al-Buriahi,M.S.(2024).Effect of Eu^{3+} ions concentration on visible red luminescence and radiative shielding properties of SrO-Al_2O_3-$BaCl_2$-B_2O_3-TeO_2 glasses,Rad.Phys.Chem.216,111467.

[10].Jose,A.,Gopi,S.,Krishnapriya,T.,Jose,T.A.,Joseph,C.,Unnikrishnan,N.V.,Biju,P.R.(2021).Spectroscopic investigations on 1.53 μm NIR emission of Er^{3+} doped multicomponent borosilicate glasses for telecommunication and lasing applications,261,124223.
[11].Meena,S.L.(2023). Structural and FTIR Analysis of Sm^{3+} ions doped Ytterbium Zinc Lithium Lead Soda lime Cadmium Phosphate Glasses,Int.J.Innov.Res.Sci.Eng.Tech.12, 10811-10820.
[12].Kumar,S.A.,Marimuthu,K.(2013).Concentration effect of Sm^{3+} ions in B_2O_3-PbO-PbF_2-Bi_2O_3-ZnO glasses-Structural and luminescence investigations,J.Alloys Comp.565,104-114.
[13].Kilic,G.,Ilik,E.,Mahmoud,K.A.,Mallawany,R.El,Agawany,El(2020).Novel zinc vanadyl borophosphate glasses:ZnO-V_2O_5-P_2O_5-B_2O_3:Physical,thermal and nuclear radiation shielding properties,Ceram.Int.46,19318-19327.
[14].Meena,S.L.(2021). Spectral and Raman Analysis of Sm^{3+}Doped in ZincLithium Soda limeAluminoSilicate Glasses,Int.J.Eng.Sci.Inv.10,28-33.
[15].Zaman,F.,Rooh,G.,Srisittipokakun,N.S.,Wongdeeying,C.,Kim,H.J.,Kaewkhao,J.(2018).Physical,structural and luminescence investigation of Eu^{3+} doped lithium gadolinium bismuth borate glasses for LEDs,Solid State Sci.18,30150.
[16].Sroda,M.,Swiontek,S.,Gieszczyk,W.,Bilski,P.(2020).The effect of lithium fluoride on the thermal stability and thermoluminescence properties of borosilicate glass and glass ceramics,J.Eur,Ceram.Soc.40,472-479.
[17].C.R.Kesavulu,H.J.Kim,S.W.Lee,J.Kaewkhao,Wantana,N.,Kothan,S.,Kaewjaeng,S.(2017).Optical spectroscopy and emission properties of Ho^{3+} doped gadolinium calcium silicate glasses for visible luminescent device applications,J.Non-Cryst.Solids,474,20-57.
[18].Prakash,M.R.,Neelima,G.,Kummara,V.K.,Ravi,N.,Viswanath,D.,Rao,T.S.,Jilani,S.M.(2019).Holmium doped bismuth-germanate glasses for green lighting applications: A spectroscopic study,Opt.Mat.94,436-443.
[19].Meena,S.L.(2024).Spectral, Thermal and Upconversion properties of Dy^{3+} doped borotellurite glasses with large stability parameter, IOSR Appl.Phys.42-49.
[20].Laxmikanth,C.,Elias,A.M.,Sichone,S.,Mwankemwa,B.(2025).Tailoringstructural,thermal and optical properties of Tm^{3+} doped borotellurite glasses through Bi_2O_3 incorporation for optical fiber construction,Next Mat.6,100274.
[21]. Meena,S.L.(2026).Spectral, Transmittance and Radiative Properties of Pr^{3+} doped Borotellurite Glasses, 10142-50.
[22].Elias,A.M.,Mwanga,S.F.,Mwankemwa,B.,Anjaiah,J.,Laxmikanth,C.(2022).Influence of Bi^{+} ions on photoluminescence properties of Tm_2O_3 doped borotellurite glasses for the near-infrared emission applications,Opt.Mat.125,112140.
[23].Meena,S.L.(2021). Spectral and Thermal properties of Pr^{3+} doped lead lithium sodium tungsten borophosphate glasses,IOSR Appl.Phys.13,1-7.
[24].Meena,S.L.(2021). Spectral and Raman Analysis of Er^{3+} doped Zinc Lithium Antimony Sodalime Tellurite Glasses,Int.J.Eng.Sci.Inv.10,09-15.
[25]. Judd, B.R. (1962). Optical Absorption Intensities of Rare Earth Ions. Physical Review, 127, 750.
[26]. Ofelt, G.S. (1962). Intensities of Crystal Spectra of Rare Earth Ions. The J. Chem. Phys., 37, 511.
[27].Sinha, S.P. (1983). Systematics and properties of lanthanides, Reidel, Dordrecht.
[28]. Krupke, W.F. (1974).IEEE J. Quantum Electron QE, 10,450.
[29].Meena, S.L.(2026).Spectral, Thermal and Raman analysis of Tm^{3+} doped in phosphate glasses for optical temperature sensor applications, IOSR Appl.Phys.18,24-30.
[30].Rai,S.B.Singh,A.K.,Singh,S.K.(2003). Spectroscopic properties of Ho^{3+} ions doped in tellurite glass, Spectrochim.Acta A,59,3221-6.
[31].Meena,S.L.(2020).Spectral and Transmittance properties of Ho^{3+} ions doped Zinc Lithium Calcium Borosilicate Glasses,Int.J.of Chem.Phy.Sci.9(6),1-9.
[32].Meena,S.L.(2022).Spectral and Upconversion properties of Ho^{3+} doped in Zinc Lithium Sodalime Cadmium Borosilicate Glasses,Int.J.Adv.Res,Sci.Eng.11(5)33-44.